Current Optics and Photonics
Vol. 1, No. 2, April 2017, pp. 118-124

ISSN: 2508-7266(Print) / ISSN: 2508-7274(Online)
DOI: https://doi.org/10.3807/COPP.2017.1.2.118

Effect of Red-emitting $Sr_{2.41}F_{2.59}B_{20.03}O_{74.8}:Eu_{0.12},Sm_{0.048}$ Phosphor on Color Rendering Index and Luminous Efficacy of White LEDs

Anh Q. D. Nguyen[1], Vinh H. Nguyen[1], and Hsiao-Yi Lee[2]*

[1]Nguyen Tat Thanh University, Ho Chi Minh 702000, Vietnam
[2]Department of Electrical Engineering, National Kaohsiung University of Applied Sciences, Kaohsiung 80778, Taiwan

(Received November 12, 2016 : revised January 9, 2017 : accepted January 31, 2017)

Color rendering index (CRI) and luminous efficacy (LE) are two key performance factors of white LEDs (WLED). While most recent works in optics focus on methodology to improve these factors, little attention has been dedicated to chemical composition of materials. This paper studies the effect of $Sr_{2.41}F_{2.59}B_{20.03}O_{74.8}:Eu_{0.12},Sm_{0.048}$ phosphor (SrSm), in terms of concentration and particle size on CRI and LE of 8500 K - WLEDs. Importantly, the molar mass of the componential ions in SrSm are calculated to shed light on the connection between the chemical composition of the material of interest and the performance of WLEDs. Results show that CRI can be improved to a value of around 86 by boosting red-light components in WLEDs, for all 3 major configurations: conformal, in-cup, and remote phosphor. CRI value tends to decrease with larger size of particles, while LE value goes in the reverse direction. On the other hand, both CRI and LE appear to be reduced at higher concentration of SrSm. This light attenuation is analyzed by using the Lambert-Beer law and Mie-scattering theory.

Keywords : White LED, Lambert-Beer law, Color rendering index, Luminous efficacy
OCIS codes : (160.4670) Optical materials; (160.4760) Optical properties; (290.4020) Mie theory; (160.2540) Fluorescent and luminescent materials

I. INTRODUCTION

Due to some remarkable progress in semiconductor physics and optoelectronics in recent years, the current generation of LEDs possesses features superior to those of traditional lighting sources, such as low power consumption, high efficiency, long life and color diversity. In particular, white LEDs are considered an ideal illumination solution to replace conventional lamps. Indeed, a WLED consists of blue-emitting base material, which is covered with another material that emits yellow light when stimulated by blue light. The mixture of blue and yellow light is perceived by human eyes as white [1-3]. Based on this principle, the color rendering index (CRI) and luminous efficacy (LE) become two key factors to the performance of WLEDs. Previous studies have confirmed that typical WLEDs require a high value of CRI (>78) to be qualified for lighting applications [4-6].

Figure 1 illustrates a conventional WLED, which consists of 9 blue LEDs and is covered by the yellow YAG:Ce^{3+} phosphor compounding (top photo). However, this original system has a poor color rendering performance (<74) due to the lack of a red light component in the spectrum [2]. Recently, the quantum dot nanophosphor and the warm-white LED has been combined to achieve a CRI value close to 90 at the correlated color temperature (CCT) of less than 3000 K [7]. Another approach is to use a pulse-sprayed conformal phosphor configuration, which is suitable for the CCT values from 2700 K to 4700 K. This approach can provide a CRI value as high as 85.6 [8]. Furthermore, a new research and development tool has been proposed to help practical designers predict the instantaneous variation in CCT and CRI when the LED system power varies. This

*Corresponding author: leehy@mail.ee.kuas.edu.tw
Color versions of one or more of the figures in this paper are available online.

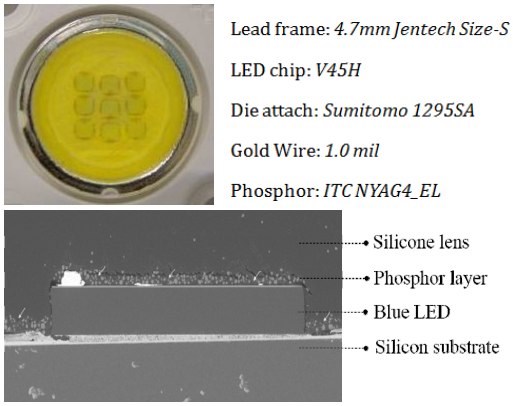

FIG. 1. The 8500 K WLED with manufacture information as a product of the Siliconware Precision Industries Co., Ltd., Taiwan (top); its SEM image of conformal phosphor layer covering a blue chip (bottom).

method can be employed for controlling CCT and CRI in future WLED packages [9]. In 2016, the green-emitting $Ce_{0.67}Tb_{0.33}MgAl_{11}O_{19}$:Ce,Tb phosphor was used to improve the CCT homogeneity and the luminous flux of multi-chip WLED lamps, at the expense of the color rendering ability [10].

In fact, although the works mentioned above propose different methods to enhance the CRI and LE performance, the results are still moderate for illumination applications. Moreover, only single-chip WLED lamps are considered in those works, hence, the results cannot be applied for multi-chip WLED lamps that have higher CCTs (>7500 K) [11, 12]. Importantly, little attention has been paid to the chemical composition of the materials involved in the manufacturing of WLEDs. Specifically, the materials are selected based on some explicit properties that have been proved in other applications, but not by rigorous analysis on their chemical composition.

$Sr_{2.41}F_{2.59}B_{20.03}O_{74.8}:Eu_{0.12},Sm_{0.048}$ (SrSm), which is a Eu-sensitized, red-emitting, and high efficiency phosphor, has been employed widely in both high-pressure and low-pressure discharge lamps due to its excellent thermal and chemical stability [13-18]. However, up to now, there have been very few studies that apply SrSm to improve the CRI of WLEDs. In this paper, we propose a novel WLED design using SrSm to enhance the CRI value up to 86. Specially, the chemical composition of SrSm is analyzed carefully by calculating the molar mass of every ion that participates in the formation of SrSm. Moreover, by means of the Lambert-Beer law and Mie scattering theory as well as Monte Carlo simulation, we demonstrate that both the concentration and the particle size of SrSm have significantly impact on the transmitted light power. As a result, we are able to keep the balance of good CRI and LE values, regardless of phosphor configuration or CCT values.

II. DETAIL OF EXPERIMENT AND SIMULATION

2.1 Composition of SrSm

The ingredients of SrSm are listed in Table 1. According to the composition of SrSm, which is described in [13], we proceed to calculate the molar percentage of each element of this chemical compound to gain insight into the formula of this mixed compound. Furthermore, the fabrication process of SrSm is also described in this section.

First, Eu_2O_3 and Sm_2O_3 particles are dissolved in a dilute nitric acid solution. Concurrently, $Sr(NO_3)_2$ and H_3BO_3 are dissolved in warm water (90°C). These 2 solutions are mixed together, after being added to a 1:1 solution of acetone and ammonium hydroxide. The whole solution is stirred vigorously. After a while, a fine white precipitate will form and become a slurry. This slurry is kept at 80°C for two hours, then cooled down to room temperature. For the next step, this precipitate is filtered and dried in air and then blended with SrF_2 and ground. The resultant is placed in an open quartz crucible and fired in air at 900°C for approximately one hour. After that, it is cooled down again, then blended and ground into fine particles. The firing process continues for two hours at 900°C, this time in a flow of H_2 in N_2 gas through the same crucible. Finally, the resultant particles are cooled and re-grinded.

2.2 Simulation process

To begin the simulation process with SrSm, we consider its emission and excitation spectra, which are presented in Fig. 2(a). According to the figure, SrSm phosphor particles emit strong red light in 684-732 nm under UV light (254

TABLE 1. Composition of red-emitting $Sr_{2.41}F_{2.59}B_{20.03}O_{74.8}:Eu_{0.12},Sm_{0.048}$ phosphor

Ingredient	Mole (%)	By weight (g)	Molar mass (g/mol)	Mole (mol)	Ions	Mole (mol)	Mole (%)
$Sr(NO_3)_2$	10.09	126.98	211.63	0.6	Sr^{2+}	0.6	0.0241
SrF_2	5.43	40.58	125.62	0.32	F^-	0.646	0.0259
H_3BO_3	84.12	309.2	61.83	5	B^{3+}	5	0.203
Eu_2O_3	0.25	5.28	351.93	0.015	O^{2-}	18.665	0.748
Sm_2O_3	0.11	2.09	348.72	0.006	Eu^{2+}	0.03	0.0012
$Sr_{2.41}F_{2.59}B_{20.03}O_{74.8}:Eu_{0.12},Sm_{0.048}$					Sm^{2+}	0.012	0.00048

nm), while SrSm phosphor exhibits rather weak emission under blue light (453 nm) or yellow-green light (555 nm). Thus, it can be expected that such combination would exhibit a low luminous efficiency due to poor excitation (250-280 nm and 300-390 nm) of SrSm phosphors. This is the reason why Sm^{2+} ion is added to SrSm, resulting in additional peaks at 395, 420 and 502 nm.

As seen from Fig. 2(b), the measured emission intensity of YAG:Ce^{3+} phosphor at 502 nm is approximately equal to 1/2 of that one at 555 nm. In that case there should be slight loss of luminous efficiency due to reabsorption. It is more important that two excitation peaks of 420 nm and 502 nm are suitable for the emission band of the considered blue chip at 416-516 nm.

The simulation covers various WLED configurations by using the commercial software package LightTools. In this process, we setup 3 configurations, including conformal phosphor package (CPP), in-cup phosphor package (IPP) and remote phosphor package (RPP) with the same average CCT of 8500 K. To guarantee that our simulation results reflect precisely the impact of the considered parameters, the real emission, absorption and excitation spectra of SrSm are first set in the LightTools program. The concentration and size of SrSm are varied to figure out suitable values to optimize key performance factors of WLEDs. The added concentration of SrSm for both CPP and RPP are the same, which ranges from 0 to 16%. Differently, the concentration of SrSm for IPP only ranges from 0 to 0.32%. This significant deviation between the SrSm concentration values in the 2 cases comes from the difference in phosphor configurations. Secondly, the other factors such as LED's wavelength, waveform, light intensity, and operating temperature are also set according to the actual WLEDs to construct the precise WLED models. These models present the best optical-thermal stability, hence, they can minimize the variations caused by nuisance parameters. To make the comparison fair, the same silicone lens and structure are used for both CPP and IPP. Specifically, we set the depth, inner and outer radius of the reflector approximately to 2 mm, 4 mm, and 5 mm, respectively. Nine LED chips are covered by either CPP or IPP, which respectively have fixed thicknesses of 0.08 mm and 2.07 mm. Each blue chip has the dimension of 1.14 mm by 0.15 mm, the radiant flux of 1.16 W, and the peak wavelength of 453 nm. This configuration is intentionally set similarly to the one in our previous study [10]. In order to maintain the same color of WLEDs when either the concentration or particle size of SrSm varies, the YAG:Ce^{3+} phosphor concentration should be changed accordingly to provide the same CCT value.

Fig. 3(a) shows that the phosphor layer of CPP is coated conformally on 9 LEDs, while in Fig. 3(b), the phosphor particles of IPP is dispersed in the silicone lens. For RPP, the phosphor layer is located at a distance to the LEDs, with the thickness of 0.08 mm, as presented in Fig. 3(c). These phosphor layers consist of YAG:Ce^{3+}, SrSm particles, and the silicone glue, which respectively have the refractive indices of 1.83, 1.93, and 1.50. In addition, an SEM image of the phosphor layer covering a blue chip is also displayed in Fig. 1(b). Here, the average radius of YAG:Ce^{3+} phosphor particles is set to 7.25 μm for all packages, which is exactly the same value as real particle size.

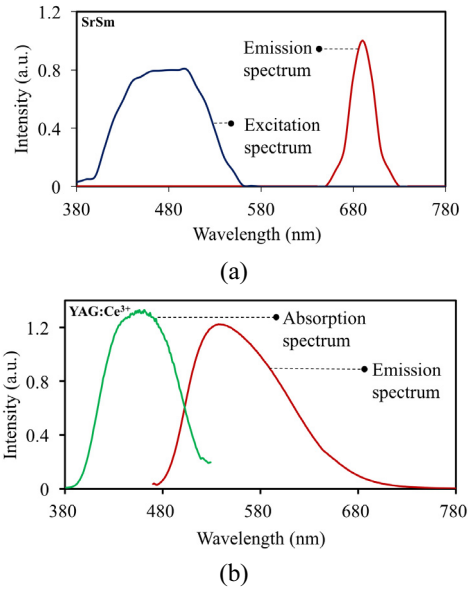

FIG. 2. (a) Emission and excitation spectra of SrSm phosphor; (b) Absorption and emission spectra of YAG:Ce^{3+} phosphor.

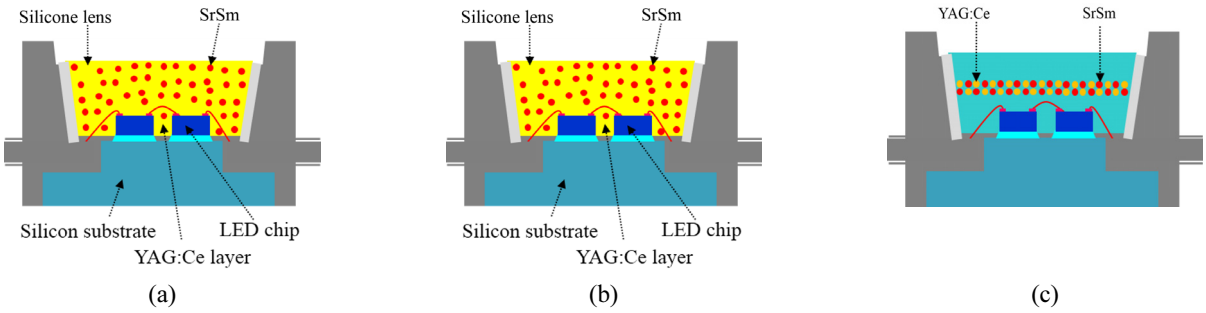

FIG. 3. Illustration of WLEDs with (a) the conformal phosphor package (CPP); (b) the in-cup phosphor package (IPP); (c) the remote phosphor package (RPP).

III. RESULTS AND DISCUSSION

In this section, LE and CRI values for various particle sizes and concentration percentages of SrSm were compared and analyzed. Firstly, the CRI values were numerically calculated and displayed on Fig. 4. Fig. 4 (top) illustrates the impact of SrSm concentration on CRI in CPP configuration. It can be observed that the CRI grows in accordance with the weight percentage of SrSm phosphor in a continuous range from 0% to nearly 10% for all SrSm particles.

The higher color rendering ability is obtained when the SrSm weight ranges from 12% to 16% with the particle size range in the 2-8 μm region. In particular, the optimal color rendering index that can be achieved exceeds 86 in this case. As for IPP configuration, the SrSm concentration ranges continuously from 0% to approximately 0.32%. For all particle sizes, the increasing of color rendering ability can be observed when the SrSm percentage ranges from 0 to 0.24%, as shown in Fig. 4 (IPP). Except for the particle size of 1 μm, the CRI value keeps increasing in the range of 0.24 to 0.32%. However, it was at the size of 1 mm that the optimal CRI of WLEDs is obtained. This value exceeds 84 for this configuration, which is 25.8% higher than the non-SrSm case, i.e. when the SrSm concentration is equal to 0%.

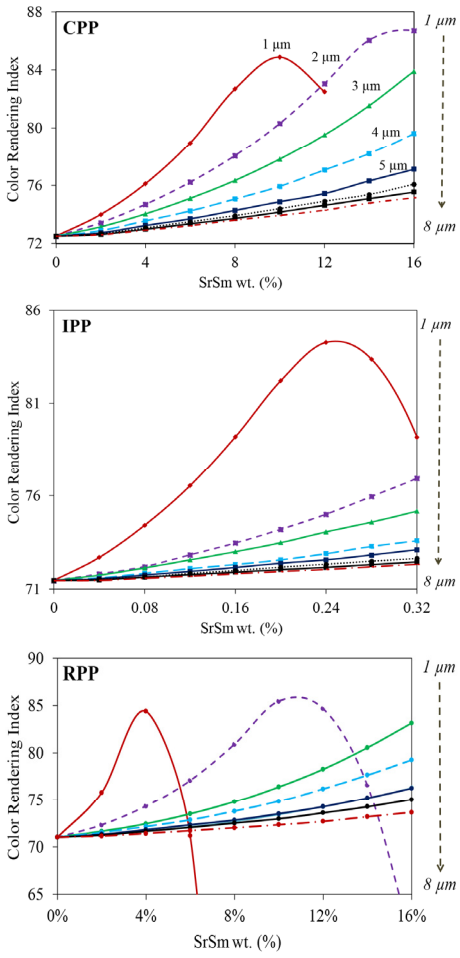

FIG. 4. Color rendering indexes of phosphor configurations corresponding to concentration and size of SrSm.

It is also indicated in Fig. 4 that the optimal CRI for RPP configuration is approximately equal to 85, which is achieved in two cases, i.e., 8% SrSm with 1 μm size and 12% SrSm with 2 μm size. For the particle sizes from 3 μm to 8 μm, the CRI value grows with the SrSm concentration. However, if the concentration and particle size of SrSm increase to beyond a certain point where the red light starts to be over dominant, the unbalance of color distribution of WLED occurs. As a result, the CRI tends to be reduced significantly after this point.

As presented in Fig. 5, the red-light spectra of two phosphor configurations, CPP and IPP, grow with the SrSm size from 1 μm to 8 μm. The plots are generated for fixed values of concentration, 12% SrSm in CPP case and 0.24% SrSm in IPP case. The deviation of red light intensity values between any two adjacent sizes from 4 μm to 8 μm is insignificant for both configurations. This is of much benefit to luminous efficacy but detrimental to the color rendering ability. Oppositely, this deviation is significant between any two adjacent sizes from 1 μm to 4 μm. Consequently, the color rendering ability should be improved significantly for 1 μm-4 μm but this creates a disadvantage for the LE. Furthermore, the emission spectra of phosphor compounds have a reduction tendency in the yellow-light band and blue-light band, causing the decreasing in luminous flux.

A more important finding from the result in Fig. 5 is

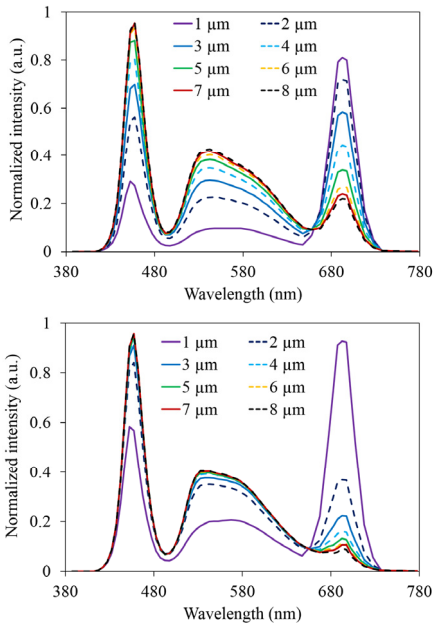

FIG. 5. The simulated emission spectrum of phosphor configurations as a function of SrSm size: (top) CPP and (bottom) IPP.

that the attenuation of emission spectrum of IPP is less severe than the one of CPP, particularly in the wavelength band of blue light and the yellow light. This implies that the luminous flux of IPP should decrease more slowly than the one of CPP when the SrSm decreases. This plays a key role in interpreting the impact of SrSm size on the luminous flux. Indeed, the simulated results demonstrate that the spectrum region of red light can be extended after mixing SrSm particles with the original phosphor compound, resulting in the improvement in color rendering ability of WLEDs.

The performance of CPP, IPP, and RPP are also illustrated in Figs. 6 and 7, which show the same phenomenon with repect to the concentration and particle size of SrSm. On one hand, the simulation confirms that CPP provides a better overall CRI than IPP and RPP do. This can be explained by the fact that the blue-yellow-red light patterns are kept synchronized, thanks to the conformal geometry of the phosphor layer. In comparison with CPP and RPP, IPP can provide higher overall LE since the phosphor composite is supported by the silicone lens, which reduces the loss due to light absorption by chips. Here, we can apply Mie-scattering theory and the Lambert-Beer law to derive the relationship between luminous output and the SrSm weight rigorously [19]. The transmitted light power can be calculated by the Lambert-Beer law [20, 21]:

$$I = I_0 \exp(-\mu_{ext} L), \tag{1}$$

where I_0 is the incident light power, L is the phosphor layer thickness (mm) μ_{ext} is the extinction coefficient, which can be expressed as $\mu_{ext} = N_r.C_{ext}$, where N_r is the number density distribution of particles (mm^{-3}). C_{ext} (mm^2) is the extinction cross-section of phosphor particles, which can be characterized by the following equation:

$$C_{ext} = \frac{2\pi a^2}{x^2}\sum_{n=1}^{\infty}(2n+1)\,\mathrm{Re}(a_n + b_n) \tag{2}$$

Here, $x = 2\pi a/\lambda$ is the size parameter, a_n and b_n are the expansion coefficients with even symmetry and odd symmetry, respectively. The parameters a_n and b_n are defined as

$$a_n(x,m) = \frac{\psi_n'(mx)\psi_n(x) - m\psi_n(mx)\psi_n'(x)}{\psi_n'(mx)\xi_n(x) - m\psi_n(mx)\xi_n'(x)} \tag{3}$$

$$b_n(x,m) = \frac{m\psi_n'(mx)\psi_n(x) - \psi_n(mx)\psi_n'(x)}{m\psi_n'(mx)\xi_n(x) - \psi_n(mx)\xi_n'(x)} \tag{4}$$

where a is the spherical particle radius, λ is the relative scattering wavelength, m is the refractive index of scattering particles, $\psi_n(x)$ and $\xi_n(x)$ are the Riccati - Bessel functions.

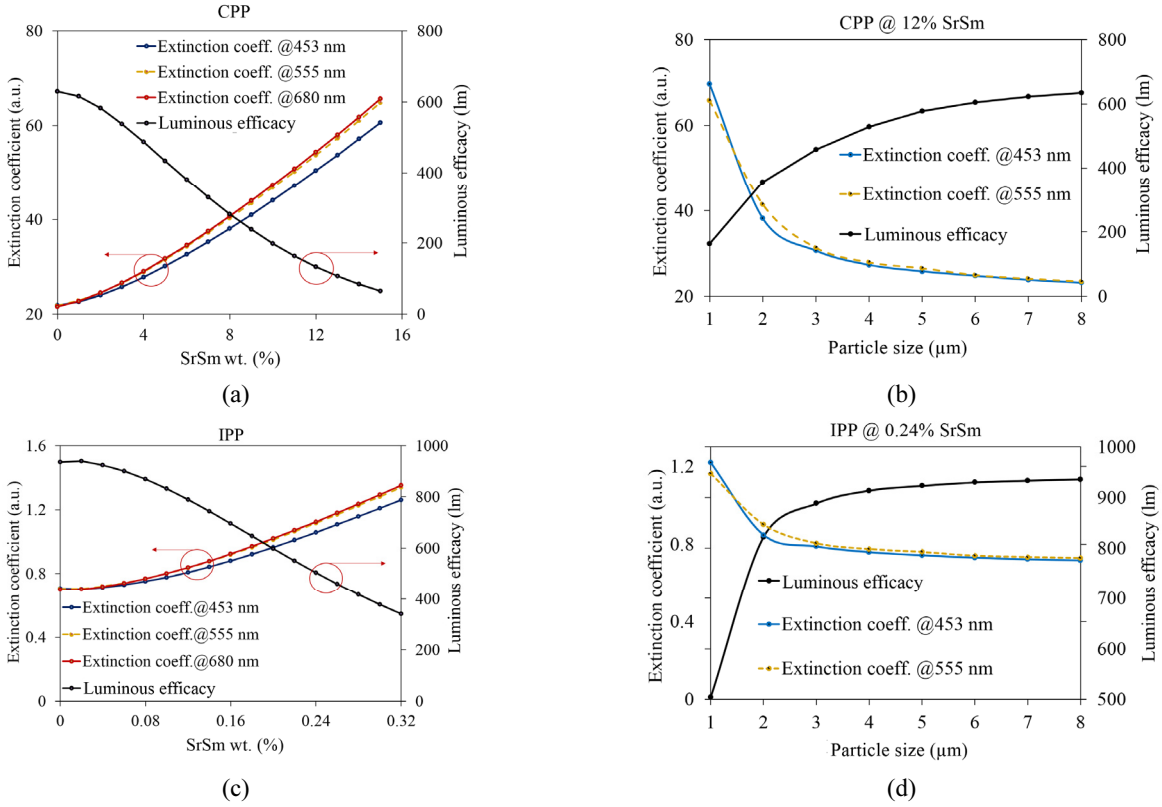

FIG. 6. Luminous efficacy and extinction coefficient of phosphor configurations corresponding to concentration and size of SrSm: (a) CPP with SrSm size of 7.25 μm. (b) CPP with 12% SrSm. (c) IPP with SrSm size of 7.25 μm. (d) IPP with 0.24% SrSm.

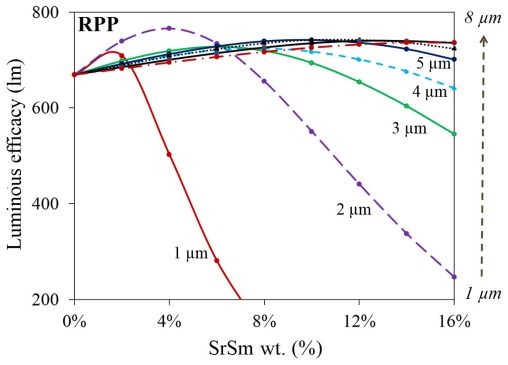

FIG. 7. Luminous efficacy of RPP corresponding to concentration and size of SrSm.

Three distinct wavelengths, 453 nm, 555 nm, and 680 nm are used to determine the extinction coefficient of the red SrSm. These 3 wavelengths are chosen because they correspond to the emission peaks of LED chips, YAG:Ce^{3+}, and SrSm phosphors, respectively. With the fixed thickness of phosphor layer for each configuration, both the number density distribution of particles N_r and the extinction cross-section C_{ext} are functions of the concentration and particle size of SrSm. Hence, transmitted light power I changes accordingly with respect to these 2 parameters.

As the SrSm particles size continuously increases from 1 μm to 8 μm, the composite becomes more and more transparent to visible light, results in less scattering and absorption, and hence, the increasing of LE and the decreasing of CRI.

According to (1), the transmitted light power grows exponentially with the decreasing of the extinction coefficient, which is a direct result of the enlargement of SrSm particle size. As a result, the higher luminous output can be emitted in comparison with the zero concentration case of SrSm (0%).

Reversely, the extinction coefficient tends to increase at higher SrSm concentration, which corresponds to the reduction of the transmitted light power I. This can be caused by the excessive addition of SrSm to the phosphor compounds, which leads to the abundant enhancement in the red light spectrum region. Meanwhile, the blue light and yellow-green light spectra decrease significantly, regardless of CPP, IPP or RPP. Consequently, lower luminous output is emitted in comparison with the non-SrSm case.

IV. CONCLUSION

In this paper, we investigate the relationship between the key performance factors of WLEDs, namely CRI and LE, and the size and concentration of SrSm for 3 configurations, i.e., CPP, IPP, and RPP. The use of SrSm in our experiment is explained by looking at the chemical formulation of this compound. In particular, we present the calculation of molar mass for every ion that participates in the formulation of SrSm. The obtained results show that the size and concentration of SrSm have contrary effects on CRI. In fact, CRI value grows with the increasing of SrSm concentration but decreases with the increasing of SrSm size. This leads to the existence of an optimal point, where CRI values can exceed 86 for CPP. Specifically, the SrSm size from 1 μm to 4 μm provides more CRI than other sizes regardless of the increasing in SrSm concentration. Oppositely, the lower LE occurs in 1-4 μm region than in 5-8 μm region. Moreover, LE should decrease significantly when adding more SrSm. This result is confirmed by analysis using Lambert-Beer law and Mie-scattering theory. Through the analysis, it can be concluded that the size and concentration of SrSm should be precisely controlled to maintain the LE and improve the CRI.

ACKNOWLEDGMENT

This research is funded by Vietnam National Foundation for Science and Technology Development (NAFOSTED) under grant number 103.03-2015.62.

REFERENCES

1. J. W. Moon, B. G. Min, J. S. Kim, M. S. Jang, K. Min Ok, K.-Y. Han, and J. S. Yoo, "Optical characteristics and longevity of the line-emitting $K_2SiF_6:Mn^{4+}$ phosphor for LED application," Opt. Mater. Express **6**, 782-792, (2016).
2. N. D. Q. Anh, M.-F. Lai, H.-Y. Ma, and H.-Y. Lee, "Enhancing of correlated color temperature uniformity for multi-chip white-light LEDs by adding SiO_2 in phosphor layer," J. Chinese Inst. Eng. **38**, 297-303 (2014).
3. B.-Y. Joo and J.-H. Ko, "Analysis of color uniformity of white LED lens packages for direct-lit LCD backlight applications," J. Opt. Soc. Korea **17**, 506-512 (2013).
4. W.-S. Sun, C.-L. Tien, J.-W. Pan, T.-H. Yang, C.-H. Tsuei, and Y.-H. Huang, "Simulation and comparison of the lighting efficiency for household illumination with LEDs and fluorescent lamps," J. Opt. Soc. Korea **17**, 376-383 (2013).
5. J. H. Oh, Y. J. Eo, S. J. Yang, and Y. R. Do, "High-Color-Quality multipackage phosphor-converted LEDs for yellow photolithography room lamp," IEEE Photonics J. **7**, 1-9 (2015).
6. P. C. Hung and J. Y. Tsao, "Maximum white luminous efficacy of radiation versus color rendering index and color temperature: Exact results and a useful analytic expression," J. Display Technol. **9**, 405-412 (2013).
7. S. Nizamoglu, T. Erdem, X. W. Sun, and H. V. Demir "Superior warm-white light-emitting diodes integrated with quantum dot nanophosphors for high luminous efficacy and color rendering," *in Proc. IEEE CLEO* (San Jose, California, USA, July 2011), pp. 1-2.
8. Z.-T. Li, Y. Tang, Z.-Y. Liu, Y.-E. Tan, and B.-M. Zhu, "Detailed study on pulse-sprayed conformal phosphor configurations for LEDs," J. Display Technol. **9**, 433-440 (2013).
9. H. Chen and S. Y. Hui, "Dynamic prediction of correlated

color temperature and color rendering index of phosphor-coated white light-emitting diodes." IEEE T. Ind. Electron. **61**, 784-797 (2014).
10. N. D. Q. Anh and H.-Y. Lee, "Improving the angular color uniformity and the lumen output for multi-chip white LED lamps by green $Ce_{0.67}$ $Tb_{0.33}$ $MgAl_{11}$ O_{19}:Ce,Tb phosphor," J. Chinese Inst. Eng. **40**, 871-875 (2016).
11. M. Schratz, C. Gupta, T. J. Struhs, and K. Gray, "Reducing energy and maintenance costs while improving light quality and reliability with led lighting technology," *in Proc. IEEE PPIC* (Charlotte, USA, June 2013), pp. 43-49.
12. H. Y. Peng, H. S. Hwang, and M. Devarajan, "Phosphor thickness effects on the optical performance of high power phosphor converted chip-on-board light-emitting diodes," *in Proc. IEEE TENSYMP* (Dalian, China, April 2014), pp. 293-296.
13. W. M. Yen and M. J. Weber, *Inorganic Phosphors: Compositions, Preparation and Optical Properties,* (CRC Press, LLC, 2000 N.W. Corporate Blvd., Boca Raton, Florida 33431, 2004).
14. Z. Qinghua, P. Zhiwu, W. Shubing, S. Qiang, and L. Shaozhe, "The luminescent properties of Sm^{2+} in strontium tetraborates (SrB_4O_7:Sm^{2+})," J. Phys. Chem. Solids **60**, 515-520 (1999).
15. K. Jang, I. Kim, S. T. Park, Y. L. Huang, H. J. Seo, and C. D. Kim, "Reduction effect on the optical properties of Sm^{2+} doped in SrB_4O_7 and SrB_6O_{10} crystals," J. Phys. Chem. Solids **67**, 2316-2321 (2006).
16. R. Komatsu, H. Kawano, Z. Oumaru, K. Shinoda, and V. Petrov, "Growth of transparent SrB_4O_7 single crystal and its new applications," J. Crystal Growth **275**, e843-e847 (2005).
17. R. Stefani, A. D. Maia, E. E. S. Teotonio, and M. A. F. Monteiro, M. C. F. C. Felinto, H. F. Brito, "Photoluminescent behavior of SrB_4O_7:RE^{2+} (*RE* = Sm and Eu) prepared by Pechini, combustion and ceramic methods," J. Solid State Chem. **179**, 1086-1092, (2006).
18. Q. H. Zeng, Z. W. Pei, S. B. Wang, and Q. Su, "The reduction of Re^{3+} in Srb_6O_{10} prepared in air and the luminescence of Srb_6O_{10}:Re^{2+} (Re=Eu, Sm, Tm)," Spectrosc. Lett. **32**, 895-912 (1999).
19. S. Liu and X. B. Luo, *LED Packaging for Lighting Applications: Design, Manufacturing and Testing,* (Chemical Industry Press and John Wiley & Sons, Beijing, 2011), Chapter 3.
20. Y. Shuai, N. T. Tran, J. P. You, and F. G. Shi, "Phosphor size dependence of lumen efficiency and spatial CCT uniformity for typical white LED emitters," IEEE ECTC., 2025-2028 (2012).
21. Z.-Y. Liu, S. Liu, K. Wang, and X.-B Luo, "Measurement and numerical studies of optical properties of YAG:Ce phosphor for white light-emitting diode packaging," Appl. Opt. **49**, 247-57 (2010).